2

The Wind and Wind Turbines

The wind is characterised by its speed and direction, which are affected by several factors, *e.g.* geographic location, climate characteristics, height above ground, and surface topography. Wind turbines interact with the wind, capturing part of its kinetic energy and converting it into usable energy. This energy conversion is the result of several phenomena that are explored in this chapter.

2.1 The Wind

This section is devoted to the study of the patterns, strengths and measured values of wind and their effects on its interaction with turbines.

2.1.1 The Source of Winds

In a macro-meteorological sense, winds are movements of air masses in the atmosphere mainly originated by temperature differences. The temperature gradients are due to uneven solar heating. In fact, the equatorial region is more irradiated than the polar ones. Consequently, the warmer and lighter air of the equatorial region rises to the outer layers of the atmosphere and moves towards the poles, being replaced at the lower layers by a return flow of cooler air coming from the polar regions. This air circulation is also affected by the Coriolis forces associated with the rotation of the Earth. In fact, these forces deflect the upper flow towards the east and the lower flow towards the west. Actually, the effects of differential heating dwindle for latitudes greater than 30°N and 30°S, where westerly winds predominate due to the rotation of the Earth. These large-scale air flows that take place in all the atmosphere constitute the geostrophic winds.

The lower layer of the atmosphere is known as surface layer and extends to a height of 100 m. In this layer, winds are delayed by frictional forces and obstacles altering not only their speed but also their direction. This is the

origin of turbulent flows, which cause wind speed variations over a wide range of amplitudes and frequencies. Additionally, the presence of seas and large lakes causes air masses circulation similar in nature to the geostrophic winds. All these air movements are called local winds.

The wind in a given site near the surface of the Earth results from the combination of the geostrophic and local winds. Therefore, it depends on the geographic location, the climate, the height above ground level, the roughness of the terrain and the obstacles in the surroundings. These are the winds the wind turbines interact with. An interesting characterisation of these surface winds is their kinetic energy distribution in the frequency domain, which is known as van der Hoven spectrum [88]. Figure 2.1 illustrates a typical spectrum. Note that the figure shows the power spectral density S_V multiplied with the angular frequency ω. Although there are some differences in detail, the spectra measured in different sites follow the same pattern. Independently of the site, the spectrum exhibits two peaks approximately at 0.01 cycles/h (4-days cycles) and 50 cycles/h (1 min cycles), which are separated by an energy gap between periods of 10 min and 2 h. The low frequency side of the spectrum corresponds to the geostrophic winds whereas the high frequency side represents the turbulence associated to the local winds.

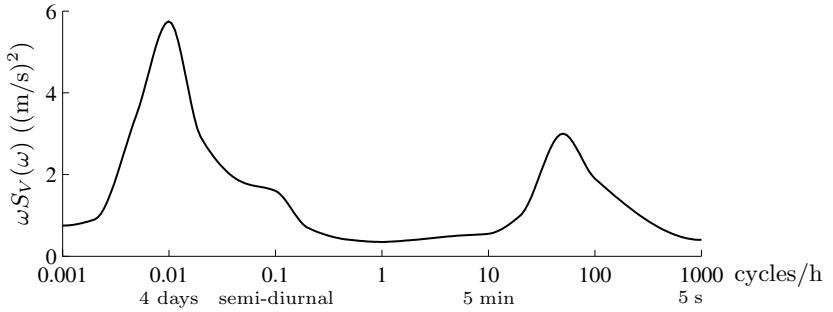

Fig. 2.1. Typical van der Hoven spectrum

The concentration of energy around two clearly separated frequencies allows splitting the wind speed signal V into two components,

$$V = V_m + v, \tag{2.1}$$

where the quasi-steady wind speed (usually called mean wind speed) V_m is obtained as the average of the instantaneous speed over an interval t_p:

$$V_m = \frac{1}{t_p} \int_{t_0 - t_p/2}^{t_0 + t_p/2} V(t) \mathrm{d}t. \tag{2.2}$$

Usually, the averaging period is chosen to lie within the energy gap, more precisely around 10 min to 20 min. When this is the case, the macro-

meteorological changes in wind speed appear as slow fluctuations of the mean wind speed, whereas the term v denotes the atmospheric turbulence.

2.1.2 Mean Wind Speed

The knowledge of the quasi-steady mean wind speeds that can be expected at a potential site is crucial to determine the economical viability of a wind energy project. These data are also essential to select the WECS in order to maximise efficiency and durability. The probability distribution of the mean wind speed is predicted from measurements collected during several years. All these data are usually arranged in a histogram. The wind distribution experimentally obtained can be approximated by a Weibull distribution, such as that shown in Figure 2.2a. The Weibull distribution is given by

$$p(V_m) = \frac{k}{C}\left(\frac{V_m}{C}\right)^{k-1} \mathrm{e}^{-(V_m/C)^k}, \tag{2.3}$$

where k and C are the shape and scale coefficients, respectively. These coefficients are adjusted to match the wind data at a particular site [91].

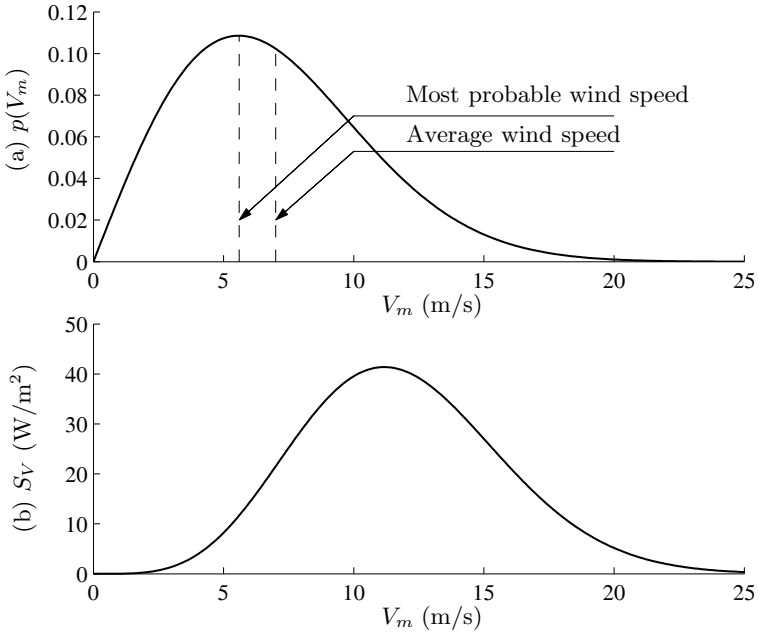

Fig. 2.2. (a) Weibull probability distribution of mean wind speeds and (b) power density vs. wind speed

The Weibull probability function reveals that large mean wind speeds rarely occur whereas moderate winds are more frequent. In the particular

case of Figure 2.2a, the most probable mean wind speed is approximately 5.5 m/s whereas the average wind speed is 7 m/s.

Mean wind speed is also function of height. The ground, even in the absence of obstacles, produces friction forces that delay the winds in the lower layers. This phenomenon, called wind shear, is more appreciable as height decreases and has important effects on wind turbine operation. Different mathematical models have been proposed to describe wind shear. One of them is the Prandtl logarithmic law [59]

$$\frac{V_m(z)}{V_m(z_{\text{ref}})} = \frac{\ln(z/z_0)}{\ln(z_{\text{ref}}/z_0)}, \tag{2.4}$$

where z is the height above ground level, z_{ref} is the reference height (usually 10 m) and z_0 is the roughness length. Typical values of this parameter for different types of terrain are listed in Table 2.1. Another empirical formula often used to describe the effect of the terrain on the wind speed gradient is the following exponential law [25]

$$V_m(z) = V_m(z_{\text{ref}}) \left(\frac{z}{z_{\text{ref}}} \right)^{\alpha}, \tag{2.5}$$

where the surface roughness exponent α is also a terrain-dependent parameter. Values of α for different types of surface are presented in the last column of Table 2.1.

Table 2.1. Typical values of roughness length z_0 and roughness exponent α for different types of surface [25, 91]

Type of surface	z_0 (mm)	α
sand	0.2 to 0.3	0.10
mown grass	1 to 10	0.13
high grass	40 to 100	0.19
suburb	1000 to 2000	0.32

2.1.3 Energy in the Wind

The kinetic energy stored in a flow per unit volume is $E_k = \frac{1}{2}\rho V^2$, where ρ is the density of the fluid. For a stream flowing through a transversal area A the flow rate is AV. Therefore, the power in the wind passing through an area A with speed V is

$$P_V = \frac{1}{2}\,\rho A V^3. \tag{2.6}$$

The energy available in the wind is obtained by integrating (2.6) during a time interval T_p, typically one year:

$$\text{Average energy} = \frac{1}{2}\,\rho A \int_0^{T_p} V^3 \mathrm{d}t. \tag{2.7}$$

One could be tempted to take the most probable wind speed or the average wind speed from the Weibull distribution and then estimate the average energy. In that case, we will really underestimate the wind resource. This is because high wind speeds contain much more energy than low wind speeds, as dictated by the cubic relation between speed and power. Figure 2.2b shows the power density, that is the distribution of energy at different wind speeds. This graph is obtained by combining the probability distribution of the wind speed with the power at each wind speed. As a result, the shape of the previous Weibull curve changes. Notice that most of the wind energy will be supplied by wind speeds above average. In Figure 2.2, the average energy corresponds to a wind speed of 11.2 m/s.

2.1.4 Turbulence

By definition, turbulence includes all wind speed fluctuations with frequencies above the spectral gap. Therefore, it contains all components in the range from seconds to minutes. In general, turbulence has a minor incidence on the annual energy capture, which is substantially determined by the quasi-steady mean wind speed. However, it has a major impact on aerodynamic loads and power quality.

Wind turbulence at a given point in space is stochastically described by means of its power spectrum. Two widely accepted models are the von Karman spectrum [46]

$$\Phi(\omega) = \frac{K_V}{(1 + (\omega T_V)^2)^{5/6}} \tag{2.8}$$

and the Kaimal spectrum [36]

$$\Phi(\omega) = \frac{K_V}{(1 + \omega T_V)^{5/3}}. \tag{2.9}$$

Both models are parameterised by constants T_V and K_V. Constant T_V determines the frequency bandwidth of the turbulence whereas K_V is associated to the turbulence power. In the time domain, T_V is also a measure of the correlation time of the turbulence. Both parameters depend on the mean wind speed as well as on the topography of the terrain. For instance, in the case of the von Karman spectrum, these coefficients are approximated by

$$K_V = 0.475\,\sigma_v^2\,\frac{L_v}{V_m(z)}, \tag{2.10}$$

$$T_V = \frac{L_v}{V_m(z)}, \tag{2.11}$$

where L_v is the correlation length of the turbulence and σ_v is the turbulence intensity defined as the ratio of turbulence power

$$\sigma_V = \sqrt{\int_{-\infty}^{\infty} \Phi(\omega) \mathrm{d}\omega} \tag{2.12}$$

to mean wind speed, *i.e.*,

$$\sigma_v \triangleq \frac{\sigma_V}{V_m(z)} \cong \frac{1}{\ln(z/z_0)}. \tag{2.13}$$

Both L_v and σ_v are specific to the terrain and are experimentally obtained from wind speed measures. The correlation length generally takes values ranging from 100 m to 330 m whereas the turbulence intensity takes values between 0.1 and 0.2.

Equation (2.13) says that turbulence intensity decreases with height. It also turns out that turbulence intensity is higher when there are obstacles in the surroundings.

2.2 The Wind Turbines

After a brief description of the types of wind rotors, we present in this section some relevant notions of aerodynamics and derive expressions for the torque and forces developed on the wind turbines.

2.2.1 Types of Rotors

Wind turbines are mechanical devices specifically designed to convert part of the kinetic energy of the wind into useful mechanical energy. Several designs have been devised throughout the times. Most of them comprise a rotor that turns round propelled by lift or drag forces, which result from its interaction with the wind. Depending on the position of the rotor axis, wind turbines are classified into vertical-axis and horizontal-axis ones.

The most successful vertical-axis wind turbine is the Darrieus rotor illustrated in Figure 2.3a. The most attractive feature of this type of turbine is that the generator and transmission devices are located at ground level. Additionally, they are able to capture the wind from any direction without the need to yaw. However, these advantages are counteracted by a reduced energy capture since the rotor intercepts winds having less energy. Furthermore, despite having the generator and transmission at ground level, maintenance is not simple since it usually requires rotor removal. In addition, these rotors are supported by guy-ropes taking up large land extensions. By these reasons, the use of vertical-axis wind turbines has considerably declined during the last decades [2, 30].

Nowadays, almost all commercial wind turbines connected to grid have horizontal-axis two-bladed or three-bladed rotors such as that drawn in Figure 2.3b. The rotor is located at the top of a tower where the winds have more energy and are less turbulent. The tower also holds up a nacelle. The gearbox and the generator are assembled inside. There is also a yaw mechanism that turns the rotor and nacelle. In normal operation, the rotor is yawed to face the wind in order to capture as much energy as possible. Although it may be very simple in low power applications, the yaw system is likely one of the more complicated devices in high power wind turbines. Finally, the power electronics are arranged at ground level. Only horizontal-axis wind turbines are treated in this book.

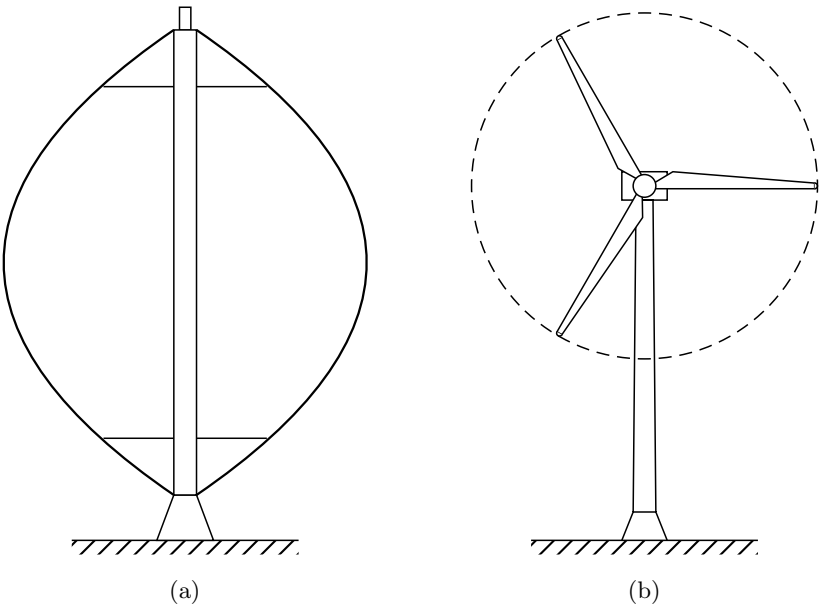

Fig. 2.3. (a) Vertical-axis and (b) horizontal-axis wind turbines

2.2.2 Wind Turbine Aerodynamics

The turbine aerodynamics describes the forces developed on a wind turbine by an airflow. The two major approaches to derive aerodynamic models for wind turbines are the actuator disc theory and the blade element theory [19, 25]. The former explains in a simple manner the energy extraction process. Also, it provides a theoretical upper-bound to the energy conversion efficiency. The latter studies the forces produced by the airflow on a blade element. This

theory is more suitable to explain some aerodynamic phenomena such as stall, as well as to study the aerodynamic loads.

Actuator Disc Model

This model is based on the momentum theory. The turbine is regarded as an actuator disc, which is a generic device that extracts energy from the wind. Consider the actuator disc is immersed in an airflow, which can be regarded as incompressible (Figure 2.4). Since the actuator disc extracts part of the kinetic energy of the wind, the upstream wind speed V is necessarily greater than the downstream speed $V_{-\infty}$. Consequently, for the stream tube just enclosing the disc, the upstream cross-sectional area A_∞ is smaller than the disc area A_D, which in turn is smaller than the downstream cross-sectional area $A_{-\infty}$. This is because, by definition, the mass flow rate must be the same everywhere within the tube

$$\rho A_\infty V = \rho A_D V_D = \rho A_{-\infty} V_{-\infty}. \tag{2.14}$$

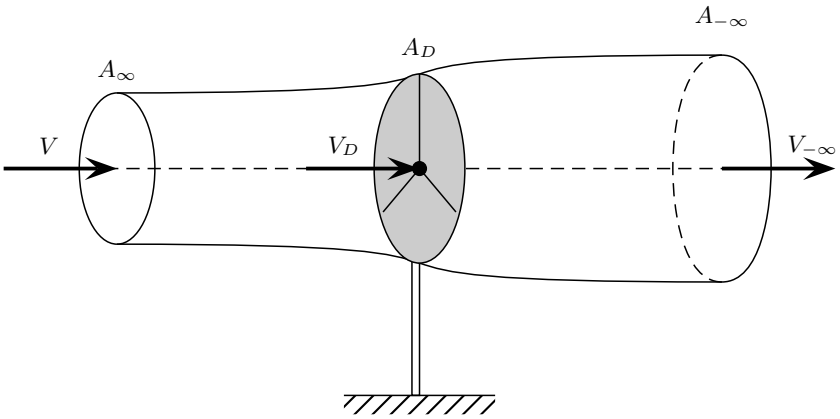

Fig. 2.4. Airflow through an actuator disc

The air that passes through the disc undergoes a speed drop $V - V_{-\infty}$. Hence, the force F_D developed by the actuator disc on the incident airflow is the total speed drop times the mass flow rate

$$F_D = (V - V_{-\infty})\rho A_D V_D. \tag{2.15}$$

Usually, the speed at the disc is written as

$$V_D = (1 - a)V, \tag{2.16}$$

where a is defined as the axial flow interference factor. The force F_D is originated by the pressure drop introduced by the actuator disc, that is,

$$F_D = (p_D^+ - p_D^-)A_D = (V - V_{-\infty})\rho A_D V(1-a), \tag{2.17}$$

where p_D^+ and p_D^- are the air pressure immediately before and after the disc. Figure 2.5 depicts how speed and pressure vary along the stream tube.

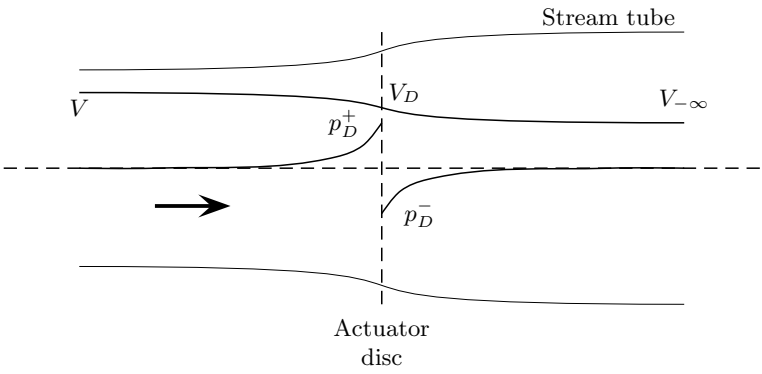

Fig. 2.5. Air speed and pressure throughout the stream tube

Bernoulli's equation is applied to obtain the pressure drop across the disc. This equation states that, under steady conditions, the total energy of the flow remains constant provided no work is done on the fluid. This equation can be applied upstream and downstream because no work is done on the fluid but for the actuator disc:

$$\frac{1}{2}\rho V_D^2 + p_D^+ + \rho g z = \frac{1}{2}\rho V^2 + p_0 + \rho g z, \tag{2.18}$$

$$\frac{1}{2}\rho V_D^2 + p_D^- + \rho g z = \frac{1}{2}\rho V_{-\infty}^2 + p_0 + \rho g z, \tag{2.19}$$

where g is the gravity, p_0 is the atmospheric pressure and the flow is regarded as horizontal. Subtracting these equations, it is obtained

$$(p_D^+ - p_D^-) = \frac{1}{2}\rho(V^2 - V_{-\infty}^2). \tag{2.20}$$

The replacement of (2.20) into (2.17) gives

$$V_{-\infty} = (1-2a)V. \tag{2.21}$$

It turns out that the momentum theory applies up to $a = 0.5$. This can be seen on noting in (2.21) that $V_{-\infty}$ becomes negative for larger values of a, what is obviously impossible.

By comparing (2.16) with (2.21), it follows that half of the speed drop occurs upstream of the disc and half downstream.

From (2.17), the force of the actuator disc on the airflow is

$$F_D = 2\rho A_D V^2 a(1-a). \tag{2.22}$$

Then, the power extracted from the wind by the actuator disc is given by

$$P_D = F_D V_D = 2\rho A_D V^3 a(1-a)^2. \tag{2.23}$$

A conventional way of characterising the ability of a wind turbine to capture wind energy is the power coefficient, which is defined as the ratio of extracted power to wind power

$$C_P \triangleq \frac{P_D}{P_V}. \tag{2.24}$$

Using (2.23) and (2.6), the power coefficient results

$$C_P = \frac{2\rho A_D V^3 a(1-a)^2}{0.5\rho A_D V^3} = 4a(1-a)^2. \tag{2.25}$$

The Betz Limit

The maximum achievable value of C_P, known as Betz limit, is $C_{P\max} = 16/27 = 0.593$ and occurs for a factor $a = 1/3$. This upper-bound applies for any type of wind turbine, even for vertical-axis ones though its derivation is different. The power coefficient of modern commercial wind turbines reaches values of about 0.45, well below the theoretical limit, though greater values have been reported for some particular designs. The power coefficient is usually provided by manufacturers. However, this data is not given as function of the interference factor a, but as function of the tip-speed-ratio and pitch angle that we will define later on.

Blade Element Model

The blade element theory is useful to derive expressions of developed torque, captured power and axial thrust force experienced by the turbine. This theory is based on the analysis of the aerodynamic forces applied to a radial blade element of infinitesimal length. To carry out the analysis, the stream tube just containing the turbine swept area is divided into concentric annular stream tubes of infinitesimal radial length, each of which can be treated independently.

Figure 2.6 illustrates a transversal cut of the blade element viewed from beyond the tip of the blade. In this figure, the aerodynamic forces acting on the blade element are also depicted. The blade element moves in the airflow at a relative speed V_{rel}, which as a first approach can be imagined as the composition of the upstream wind speed V and the tangential blade element speed $\Omega_r r$. In a later paragraph, some corrections will be introduced to account for the local flow variations caused by the turbine. Anyway, how V_{rel} is actually composed is immaterial for the moment. The airflow establishes a differential

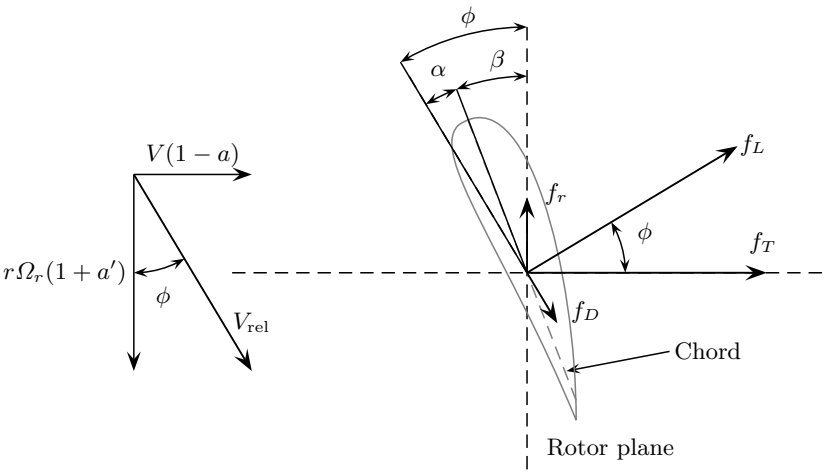

Fig. 2.6. Forces on a blade element

pressure around the blade element, which results in a force perpendicular to the local air movement direction, the so-called lift force f_L. Additionally, a drag force f_D is done in the flow direction.

The lift and drag forces per unit length are generally expressed in terms of the lift and drag coefficients C_L and C_D:

$$f_L = \frac{\rho c}{2} V_{\text{rel}}^2 C_L(\alpha), \tag{2.26}$$

$$f_D = \frac{\rho c}{2} V_{\text{rel}}^2 C_D(\alpha), \tag{2.27}$$

where c is the chord length of the blade element. Both lift and drag coefficients are functions of the incidence angle α defined as the angle that the flow makes with the chord. As observed in Figure 2.6,

$$\alpha = \phi - \beta, \tag{2.28}$$

where ϕ is the angle between the local flow direction and the rotor plane and the so-called pitch angle β is measured between the chord and the rotor plane. Note that the chord length and the pitch angle may vary along the blade, *i.e.*, they may be functions of the radial distance r of the blade element to the axis of rotation.

Figure 2.7 plots typical shapes of coefficients $C_L(\alpha)$ and $C_D(\alpha)$ of an aerofoil [91]. For low incidence angles, it is observed that C_L increases in proportion to α whereas $C_D(\alpha)$ remains almost constant and very low. However, an abrupt change occurs at $\alpha \cong 13^{\text{o}}$. When the incidence angle exceeds this critical value, the airflow is no more laminar and separates from the upper side of the aerofoil. This yields a differential pressure that reduces the lift and increases the drag. Under these conditions, it is said that the aerofoil stalls.

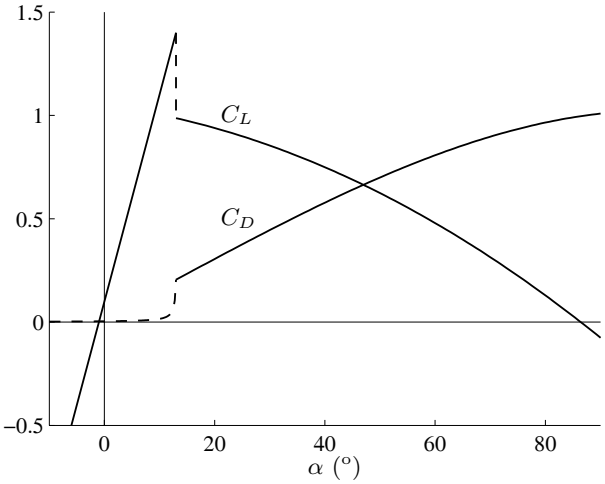

Fig. 2.7. Typical drift and drag coefficients of an aerofoil [91]

The lift and drag forces can be resolved into axial and tangential components. The former is called axial thrust force, and can be expressed per unit length as

$$f_T = \frac{\rho c}{2} V_{\text{rel}}^2 \left(C_L(\phi - \beta)\cos(\phi) + C_D(\phi - \beta)\sin(\phi) \right). \tag{2.29}$$

This thrust force must be supported by the rotor, tower and foundations. On the other hand, the tangential force develops a rotational torque that produces useful work. This torque per unit length is given by

$$\tau_r = \frac{\rho c}{2} V_{\text{rel}}^2 r \left(C_L(\phi - \beta)\sin(\phi) - C_D(\phi - \beta)\cos(\phi) \right). \tag{2.30}$$

Both lift and drag forces contribute to the axial thrust force. Further, the lift force develops useful torque whereas the drag opposes it. So, a high ratio C_L/C_D is desirable to achieve high conversion efficiency. In fact, the higher the ratio C_L/C_D, the higher will be the useful work. During stall, an abrupt drop of this ratio takes place. This is the basis for one of the most common methods to limit the captured power at winds exceeding the rated wind speed of the turbine.

To compute the contribution of each blade element to the global thrust force and rotational torque, the magnitude and direction of the relative air movement are needed. Therefore, let us redirect our attention to the relative speed V_{rel}. The analysis based on the actuator disc model showed that the airflow undergoes an overall speed drop $2aV$ (see Equation 2.21) and that half this speed drop occurs upstream so that the actual stream-wise speed at the disc is given by (2.16). Additionally, when the ideal actuator disc is replaced by a real turbine having a finite number of blades, the airflow suffers

a change in its direction produced by the blade elements as reaction to the aerodynamic torque. This explains the helical wake that arises downstream of the turbines, which results from the superposition of the stream-wise speed and the rotational speed induced by the blades. The change in tangential speed is usually expressed as function of the tangential flow induction factor a'. Upstream of the disc the flow is axial, *i.e.*, its rotational speed is zero. Immediately downstream of the rotor area, the rotational speed is $2\Omega_r a'$. It is assumed that the rotational speed at the blade chord line is $\Omega_r a'$. Thus, the relative speed V_{rel} can be expressed as

$$V_{\text{rel}} = V\sqrt{(1-a)^2 + \left(\frac{r\Omega_r}{V}(1+a')\right)^2}, \tag{2.31}$$

$$\tan(\phi) = \frac{V}{\Omega_r r}\frac{1-a}{1+a'}. \tag{2.32}$$

Note that the magnitude and direction of the relative wind speed vary along the blade span. Also, a and a' are generally not uniform over the blades.

2.2.3 Force, Torque and Power

The thrust force acting on the entire rotor and the total useful torque developed by the turbine are obtained by integrating (2.29) and (2.30) along the blades length. Commonly, thrust force, torque and power are expressed in terms of non-dimensional thrust (C_T), torque (C_Q) and power (C_P) coefficients as follows

$$F_T = \frac{1}{2}\rho\pi R^2 C_T(\lambda,\beta)V^2, \tag{2.33}$$

$$T_r = \frac{1}{2}\rho\pi R^3 C_Q(\lambda,\beta)V^2, \tag{2.34}$$

$$P_r = C_P(\lambda,\beta)P_V = \frac{1}{2}\rho\pi R^2 C_P(\lambda,\beta)V^3, \tag{2.35}$$

where C_P and C_Q satisfy

$$C_Q = C_P/\lambda. \tag{2.36}$$

Note that the three coefficients are written in terms of the pitch angle and the so-called tip-speed-ratio λ defined as

$$\lambda = \frac{\Omega_r R}{V}. \tag{2.37}$$

This parameter is extremely important and, together with β in the case of variable-pitch rotors, determines the operating condition of a wind turbine. Hereafter, we use β to denote pitch angle deviations introduced by pitch actuators in the case of variable-pitch wind turbines.

The torque and power coefficients are of special interest for control purposes. Figure 2.8 shows typical variations of C_Q and C_P with the tip-speed-ratio and the pitch angle deviation. In the case of fixed-pitch wind turbines, C_Q and C_P vary only with λ, since $\beta = 0$ naturally. So, with some abuse of notation we will write $C_Q(\lambda)$ and $C_P(\lambda)$ to denote $C_Q(\lambda, 0)$ and $C_P(\lambda, 0)$, respectively. Figure 2.9 depicts typical coefficients $C_Q(\lambda)$ and $C_P(\lambda)$ of fixed-pitch turbines in two-dimensional graphs.

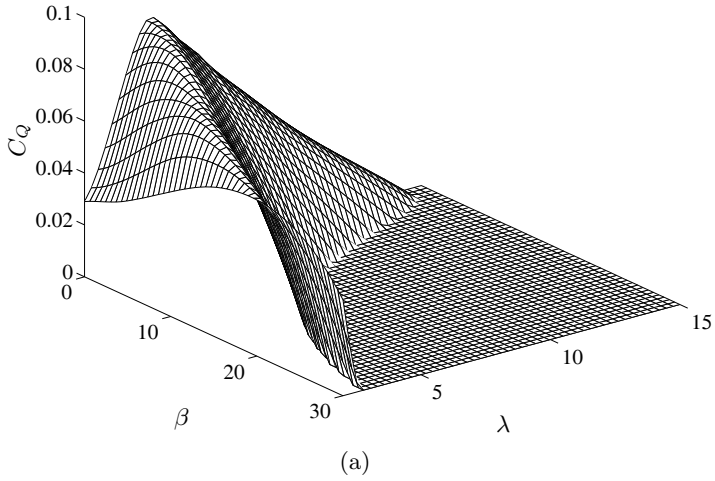

(a)

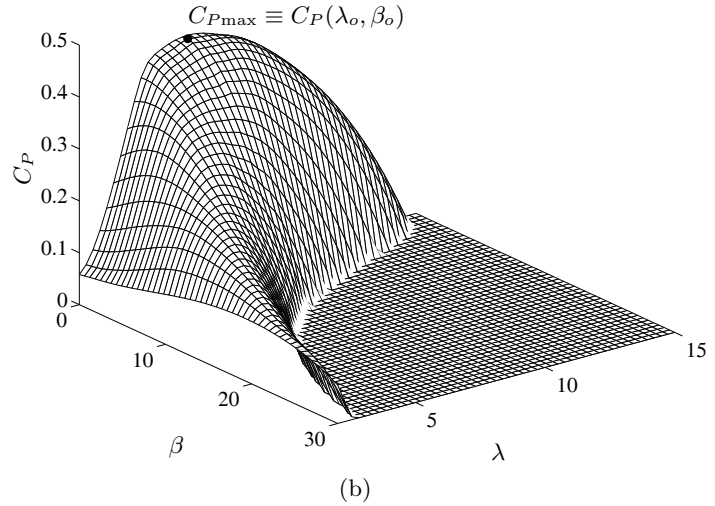

(b)

Fig. 2.8. Typical variations of (a) C_Q and (b) C_P for a variable-pitch wind turbine

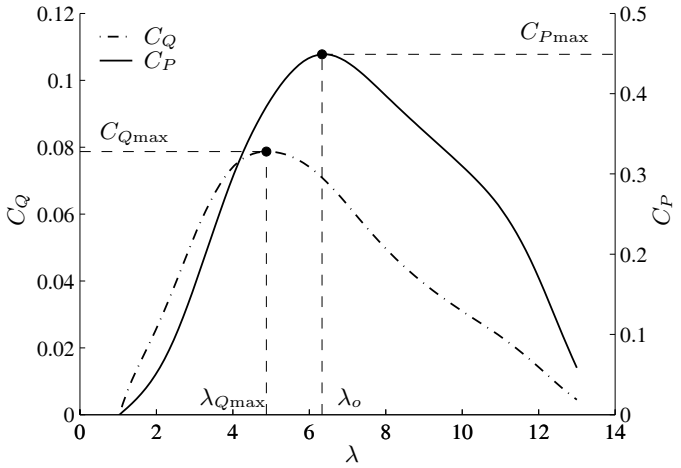

Fig. 2.9. Typical variations of C_Q and C_P for a fixed-pitch wind turbine

The power coefficient C_P has its maximum at (λ_o, β_o), with β_o being a very small angle, ideally zero. This has a pair of important connotations. On the one hand, the maximum at $\beta \cong 0$ means that any deviation of the pitch angle yields lower power capture. On the other hand, maximum conversion efficiency is accomplished at λ_o. So, fixed-speed turbines will operate with maximum efficiency just for a unique wind speed, whereas variable-speed turbines can potentially work with maximum efficiency over a wide wind speed range at least up to rated power. To realise the potential benefits of variable-speed operation, the rotational speed must be adjusted initially in proportion to the wind speed to maintain an optimum tip-speed-ratio. It can also be observed that the maximum of C_Q occurs at $(\lambda_{Q\max}, \beta_o)$, with $\lambda_{Q\max} < \lambda_o$.

Figures 2.10 and 2.11 show aerodynamic torque and power vs. rotor speed with the wind speed and the pitch angle as parameters, respectively. The thick line plots the locus of maximum power efficiency ($\lambda = \lambda_o$). It is observed that maximum torque and maximum power occur at different rotor speeds. More precisely, maximum torque occurs at lower speeds.

2.3 Wind Speed Experienced by the Turbine

Up to now, we have used V to represent the wind speed. However, the wind speed distribution is far from being uniform throughout the area swept by the blades of a wind turbine (observe that the rotor area may well exceed 10^3 m^2). Figure 2.12 illustrates a typical three-dimensional wind field. Wind speeds measured at different points of the swept area may substantially differ, both in its mean and turbulent components.

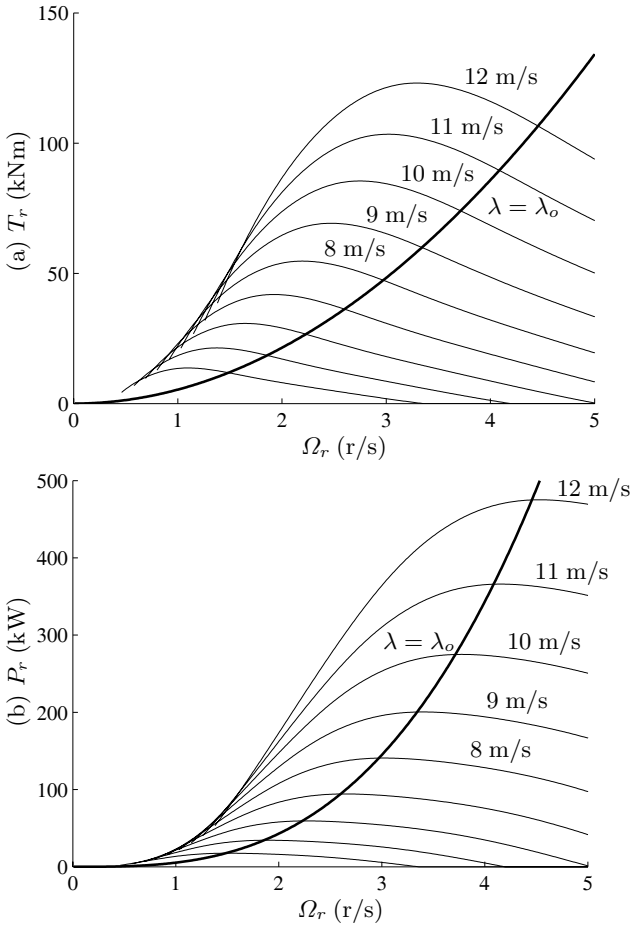

Fig. 2.10. (a) Torque and (b) power vs. rotor speed with wind speed as parameter and $\beta = 0$

As a consequence of this spatial distribution, a blade element $\mathbf{s_r}$ will experience different wind speeds as it rotates. As a first approach, let us assume that the wind speed is frozen, *i.e.*, that the wind speed at each point remains constant during a revolution. In that case, the wind speed experienced by $\mathbf{s_r}$ will be a periodical signal with fundamental frequency equal to the rotational speed. This frequency is denoted as 1P. This fluctuation of the wind speed experienced by a rotating point is called rotational sampling. It produces cyclic perturbations to the aerodynamic thrust force and rotational torque that must be supported by the blades. Furthermore, some frequency components of these perturbations, more precisely those of frequencies integers of NP, with N being the number of blades, propagate down the drive-train and structure. These aerodynamic loads have a direct impact on the cost of

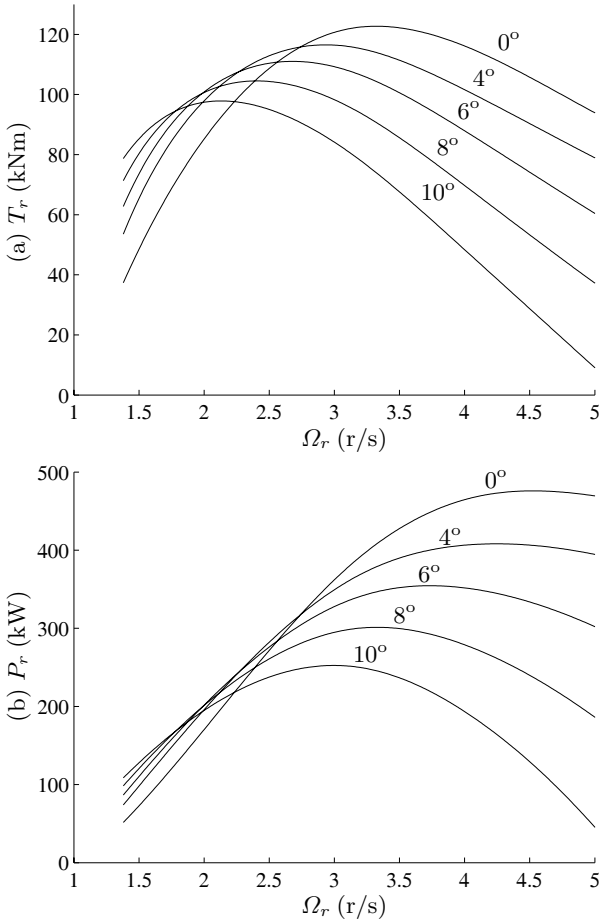

Fig. 2.11. (a) Torque and (b) power vs. rotor speed with pitch angle as parameter and $V = 12$ m/s

energy. In fact, they reduce the useful life of the WECS and deteriorate the quality of the power supplied to the grid. Increasingly, modern wind turbines include control systems that mitigate these loads.

As already discussed in Section 2.1, the wind speed at a fixed point can be split into the quasi-steady mean speed and the turbulence, where the mean speed is typically determined as a 10 min to 20 min average value. Therefore, we can regard the mean wind speed as constant during a revolution. The speed variation at a rotating point can be separated into a deterministic and a stochastic component. The former is due to the spatial distribution of the mean speed whereas the latter is due to the turbulence. On the one hand, the factors that contribute to the deterministic component are primarily wind shear, tower shadow and the presence of other wind turbines and obstacles in

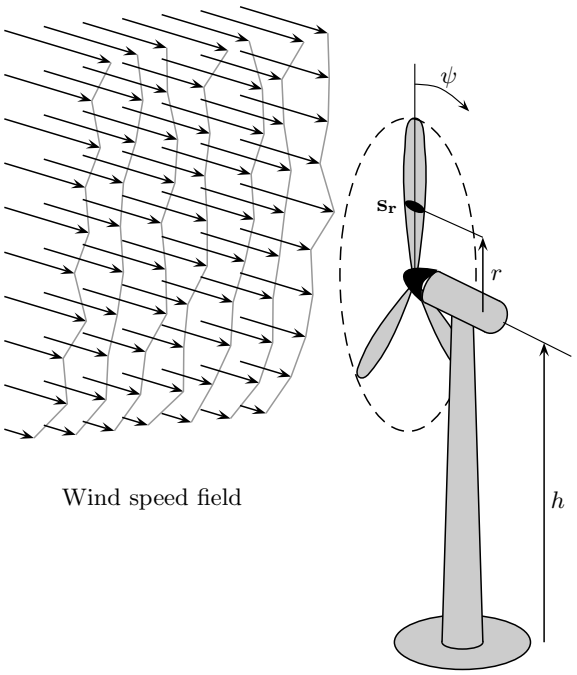

Fig. 2.12. Spatial distribution of the wind passing through the area swept by the turbine

the surroundings. On the other hand, the stochastic component is caused by the temporal and spatial distribution of the turbulence.

2.3.1 Deterministic Component

We describe here the main causes of deterministic wind fluctuations, *i.e.*, wind shear and tower shadow [19, 63].

Wind Shear

The increase of mean wind speed with height is one of the causes of aerodynamic loads. In fact, the mean speed gradient produces a cyclic variation in the wind speed experienced by a rotating blade element (see Figure 2.12). For instance, the wind speed faced by $\mathbf{s_r}$ coincides with the mean wind speed at the hub when the blade is horizontal ($\psi = \pm\pi/2$), is lower when the blade is downwards ($\psi = \pi$), and is higher when the blade is upwards ($\psi = 0$). To quantify this wind speed variation, we use one of the expressions given in Section 2.1.2 to describe the wind speed gradient. The height above ground of the blade element $\mathbf{s_r}$, h_r, varies with the angle ψ as

$$h_r = h - r\cos(\psi), \tag{2.38}$$

where h is the height of the tower and r is the distance from the blade element $\mathbf{s_r}$ to the axis of rotation. Then, replacing the generic height z with the blade element height h_r into (2.4) and using the tower height h as reference height, it follows

$$V_m(h_r) = V_m(h)\frac{\ln\left(\dfrac{h - r\cos(\psi)}{z_0}\right)}{\ln\left(\dfrac{h}{z_0}\right)}. \tag{2.39}$$

The cyclic torque fluctuations caused by wind shear are depicted in Figure 2.13. The torque fluctuation of each blade is nearly sinusoidal with fundamental frequency 1P. Due to the averaging effect of the blades, just frequency 3P and harmonics are propagated down the hub, transmission and generator whereas the fundamental component is cancelled. Thus, the aerodynamic loads on the blades are significantly attenuated when transmitted through the remaining devices of the drive-train. Wind shear effect is much more appreciable in two-bladed turbines.

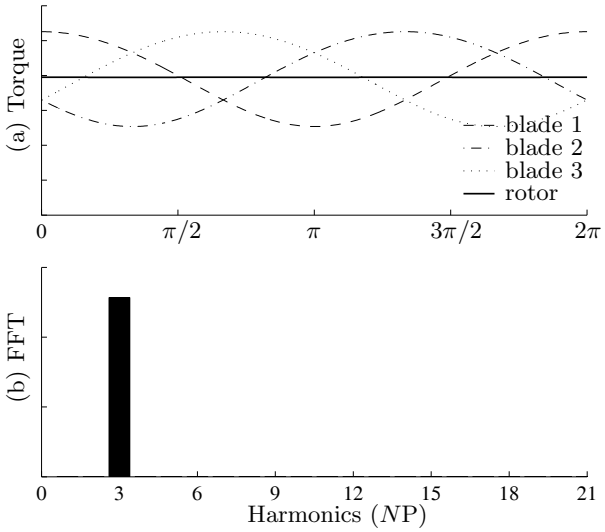

Fig. 2.13. Wind shear effect ($N = 3$): (a) Normalised torque fluctuations of each blade and rotor, (b) Fast Fourier Transform of the rotor torque

Tower Shadow

Horizontal-axis wind turbines always have a tower supporting the rotor, transmission and generator. This tower may be tubular in the case of small-scale

turbines and are cylindrical in medium to ones. Towers are obstacles that affect appreciably the airflow. Although some down-wind designs were developed in the past to simplify the yaw mechanism, modern wind turbines have the rotor upstream of the tower. It is illustrated in Figure 2.14 how the streamlines deviate just in front of the tower of an up-wind turbine. The airflow takes a lateral speed whereas its axial speed decreases. This effect is called tower shadow.

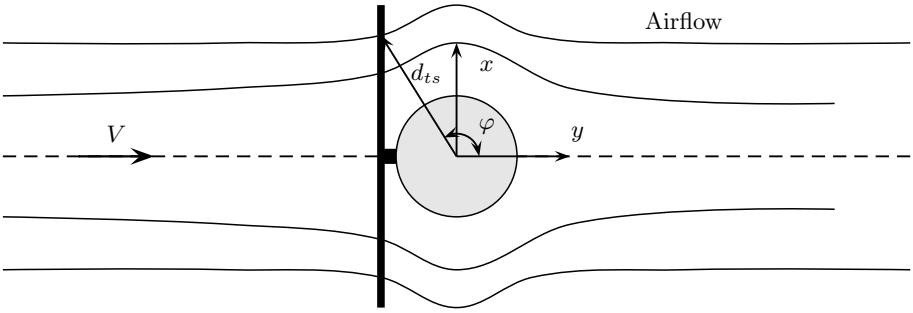

Fig. 2.14. Effect of tower shadow on the airflow

Just a rough estimation of the tower shadow effect is presented here. To this end, let us approximate the tower to a cylinder immersed in a two-dimensional air flow. Then, the following expressions for the axial (V_y) and lateral (V_x) components of the wind speed experienced by the blade element $\mathbf{s_r}$ can be derived:

$$V_x = \begin{cases} V\left(\dfrac{r_t^2}{d_{ts}^2}\right)\sin(2\varphi) & \pi/2 \le \psi < -\pi/2, \\ 0 & -\pi/2 \le \psi < \pi/2, \end{cases} \tag{2.40}$$

$$V_y = \begin{cases} V\left(1 - \dfrac{r_t^2}{d_{ts}^2}\cos(2\varphi)\right) & \pi/2 \le \psi < -\pi/2, \\ V & -\pi/2 \le \psi < \pi/2, \end{cases} \tag{2.41}$$

where r_t is the tower radius, d_{ts} is the distance from $\mathbf{s_r}$ to the centre of the tower and φ is the angle between $\mathbf{s_r}$ and the y-axis. Note that the airflow deviation is only appreciable in the lower half of the swept area.

Draft and lift are primarily affected by V_y. Figure 2.15 shows the effects of tower shadow on the torque developed by a three-bladed wind turbine. The fast Fourier transform depicted in the lower part of the figure reveals that the energy spreads over a wide range of frequencies. It is observed that the 3P component is more appreciable than in the wind shear effect. In general, tower shadow is the most important deterministic load. It is worthy to mention that

the 'shadow' caused by other obstacles, such as plants, buildings or other wind turbines, has similar effects and can be treated likewise, though the quantification may result much more involved.

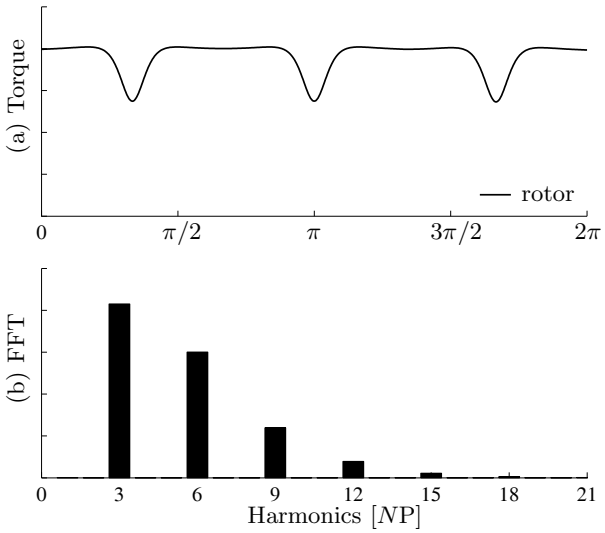

Fig. 2.15. Tower shadow effect ($N = 3$): (a) Normalised rotor torque fluctuations and (b) Fast Fourier Transform

2.3.2 Stochastic Component

In addition to the deterministic fluctuations, there is a stochastic variation of the wind speed at a rotational point. The turbulence spectrum observed by a rotating blade element will differ from the spectrum at a fixed point. In fact, part of the energy in the turbulence will move towards higher frequencies and will concentrate around integers of frequency 1P. To what extent the energy will be transferred from the stationary spectrum to integers of the rotor speed will mainly depend on the rotational frequency, the distance of the blade element to the hub, the turbulence bandwidth and the correlation length. The turbulence experienced by a rotor is sometimes called rotational turbulence.

To illustrate clearly this effect, assume for the moment that the rotational frequency is much higher than the turbulence bandwidth, thereby we can imagine the wind field is frozen. Then, a rotating blade element will experience a cyclic wind fluctuation. So, the corresponding power spectrum will consist of impulses at integers of frequency 1P. The amplitude of this fluctuation will be larger for blade elements near the tip and lower for blade elements

near the hub. In the limit, the centre of the rotor observes the same wind speed regardless whether it is rotating or not. This has to do with the correlation length of the turbulence. In fact, as the ratio r/L_v increases, the correlation among the wind speeds around a revolution decreases. So, the rotational sampling will be more appreciable for terrains having a low correlation length. Let us now unfreeze the wind field. As rotor speed decreases, the energy in the impulses spreads out. In the limit, if the rotational speed were comparatively very low, there would not be any difference between the power spectra at a fixed point and at a rotating point.

In real wind turbines, the rotational frequency may be several times higher than the turbulence bandwidth. So, the wind experienced by the blades will have high energy concentrated around 1P and harmonics. It is remarked that these cyclic wind perturbations are higher in the outer part of the rotor, which precisely more contributes to the aerodynamic torque. Therefore, the aerodynamic torque developed by the entire rotor will have appreciable fluctuations of frequencies around NP. Rotational sampling of turbulence has been reported as the main cause of flicker in grid-connected wind turbines [76].

http://www.springer.com/978-1-84628-492-2

Wind Turbine Control Systems
Principles, Modelling and Gain Scheduling Design
Bianchi, F.D.; de Battista, H.; Mantz, R.J.
2007, XX, 208 p., Hardcover
ISBN: 978-1-84628-492-2